HHS Public Access

Author manuscript

Trans Soc Min Metall Explor Inc. Author manuscript; available in PMC 2015 September 18.

Published in final edited form as:

Trans Soc Min Metall Explor Inc. 2013 January ; 332: 505–513.

Computational fluid dynamics (CFD) investigation of impacts of an obstruction on airflow in underground mines

L. Zhou, **G. Goodman**, and **A. Martikainen**

Office of Mine Safety and Health Research, National Institute for Occupational Safety and Health, Pittsburgh, PA

Abstract

Continuous airflow monitoring can improve the safety of the underground work force by ensuring the uninterrupted and controlled distribution of mine ventilation to all working areas. Air velocity measurements vary significantly and can change rapidly depending on the exact measurement location and, in particular, due to the presence of obstructions in the air stream. Air velocity must be measured at locations away from obstructions to avoid the vortices and eddies that can produce inaccurate readings. Further, an uninterrupted measurement path cannot always be guaranteed when using continuous airflow monitors due to the presence of nearby equipment, personnel, roof falls and rib rolls. Effective use of these devices requires selection of a minimum distance from an obstacle, such that an air velocity measurement can be made but not affected by the presence of that obstacle. This paper investigates the impacts of an obstruction on the behavior of downstream airflow using a numerical CFD model calibrated with experimental test results from underground testing. Factors including entry size, obstruction size and the inlet or incident velocity are examined for their effects on the distributions of airflow around an obstruction. A relationship is developed between the minimum measurement distance and the hydraulic diameters of the entry and the obstruction. A final analysis considers the impacts of continuous monitor location on the accuracy of velocity measurements and on the application of minimum measurement distance guidelines.

Keywords

Mine ventilation; Airflow measurement; Obstruction; Continuous airflow velocity monitoring; Computational fluids dynamics (CFD)

Introduction

The proper control and distribution of ventilation air are key considerations in improving the health and safety of underground mine workers (Thimons and Kohler, 1985). Continuous monitoring of airflow velocity is one means of accomplishing this. While transverse plane handheld anemometers can be moved to avoid airflow obstructions that can affect measurement accuracy, continuous readings are typically made only at fixed positions and,

at times, may be influenced by nearby obstructions. Effective use of continuous airflow monitoring requires knowledge of the minimum measurement distance, beyond which the effects of vortices and eddies are reduced, allowing for accurate measurement of airflow velocities. According to Kohler and English (1983), much attention has been focused on this problem, with recommendations first reported as early as 1926. Unfortunately, the widely varying suggestions, such as recommended measurement locations from 10 to 100 entry diameters downstream of obstructions, are too broad to be of help (Kohler and English, 1983). A criterion specifying the minimum downstream distance at which a measurement can be made from an obstruction would be very helpful. Kohler and English (1983) and Thimons and Kohler (1985) recommended that measurements at locations near obstructions or changes in the air course should be avoided when possible, and that measurements should always be made at minimum distances of three entry diameters upstream and ten entry diameters downstream of the obstruction if it is unavoidable. The authors also stated that downstream effects of obstructions or changes are much more pronounced than upstream effects; consequently, measurements should be obtained on the upstream side of the obstructions.

In the above recommendations, entry size is taken as the only factor affecting measurement distance. However, the size of the obstruction could also influence the minimum distance, as a larger obstruction could produce a larger disturbed area downstream than a smaller-sized obstruction. In addition, the incident airflow velocity could have an effect on the airflow downstream of the obstruction. Therefore, identifying the factors influencing the minimum downstream measurement distance is critical for proper interpretation of output from continuous airflow monitors. Thus far, no comprehensive analysis on how an obstruction affects the minimum distance has been performed in mining research.

Computational fluids dynamics (CFD) is a widely used technique for modeling and understanding the behavior of fluids. Increased computer power in the last decade has been a dominant factor in determining the rapid growth of industrial utilization of this technique. CFD modeling is the process of representing a fluid flow problem by way of fundamental governing equations of fluid dynamics, which are based on the laws of conservation of mass and momentum. CFD can be easily coupled to modern tools for three-dimensional visualization and for creating maps of velocity vectors, streamlines, iso-value contours, etc. By running a CFD analysis of a dynamic fluid flow, an analyst can gain insight into the dynamic behavior of a physical system that is otherwise often very difficult, time-consuming and expensive to achieve using experimental methods.

A growing number of CFD studies have been performed in mine ventilation research, due to its significant advantages, which include illustrative presentation of results and its use as an alternative to expensive, time-consuming or difficult experimentation. Gong and Bhaskar (1992) developed a three-dimensional mathematical model to evaluate airflow fields at a continuous miner face. Hargreaves and Lowndes (2007) constructed a series of steady-state CFD models to replicate the ventilation flow patterns seen at the end of a continuous miner face during the various stages of a cutting and bolting cycle. Aminossadati and Hooman (2008) used CFD modeling to investigate the effects of brattice length on fluid flow behavior in underground crosscut regions. Wala et al. (2007) conducted a validation study of

CFD code by comparing its results against mining-related benchmark experimental data, with the conclusion that CFD is a useful method for the analysis of underground mine face ventilation systems.

Although no CFD studies have been done regarding the impact of obstructions on minimum measurement distance, there are a great number of studies in the field of wind and mechanical engineering (Lu et al., 1999; Sahini, 2004; Konno et al., 2009; Izadi et al., 2009; Dhiman and Hasan, 2010; Tavakol and Yaghoubi, 2010; Meile et al., 2011) that have demonstrated the successful use of CFD to investigate the movement of airflow around obstructions.

In this paper, a CFD model was created to investigate the impact of an obstruction on the output of an anemometer located in an underground mine entry. This model was subsequently validated with experimental test results obtained from underground testing. Parameters such as incident air velocity, obstruction size and entry size were evaluated for their potential impacts on the output of this anemometer. Criteria were also specified for locating a continuous recording anemometer to minimize measurement inaccuracies.

Validation of the CFD model

As a numerical solution method for complex, real problems, CFD cannot avoid necessary engineering simplifications and mathematical approximations. The CFD model needs to be well validated against a range of relevant experimental data before it can be successfully applied to further analyses. To address this need, a series of underground tests were conducted at the U.S. National Institute for Occupational Safety and Health (NIOSH) Bruceton Experimental Mine to study the effects of obstructions on the readings of ultrasonic anemometers (Martikainen et al., 2011). The current work uses these experimental test results to validate the CFD model for the study of obstruction effects.

Experimental tests

Three tests were conducted at the NIOSH Bruceton Experimental Mine (Fig. 1) to study the impact of obstructions on ultrasonic anemometer readings (Martikainen et al., 2011). Testing occurred at a location (location 1) in a long, straight section of a tunnel with a cross-sectional area of 5.3 m^2 (57 ft^2). The second location (location 2) is in a curve of about 45°. Location 3 is in an entry to an opening used to run cables through a bulkhead. The cross sectional area of location 3 is 3.0 m^2 (32 ft^2), and the cross sectional area of the opening is 0.7 m^2 (7.5 ft^2).

An electrician's personnel and equipment carrier cart was placed at location 1 and location 2 to examine the impacts of this stationary obstruction on airflows. Due to the smaller cross sectional area of location 3, no obstruction was presented for the ultrasonic anemometer airflow measurements.

Comparing location 1 and location 2, the latter is at a 45° bend where the airflow direction and flow pattern will vary as air moves through the bend. The air velocity measurements at location 2 were influenced not only by the presence of an obstruction in the airstream, but also by the changes in flow direction. The test results at location 1 were not affected by

changes in air course (bends, intersections, etc.) but only by the presence of the obstruction. Therefore, location 1 is the best choice among the three testing locations for constructing a CFD model to investigate the influence of an obstruction on airflow measurements.

During the testing at location 1, two-axis ultrasonic anemometers were placed on both sides of the entry with the three-axis ultrasonic anemometer set in the middle (Fig. 2). The cart obstruction was placed 3 m (9.8 ft) upstream of the anemometers in the middle of the entry. Six two-axis ultrasonic readings were made on each side of the entry, with one three-axis ultrasonic reading made in the middle. The two-axis velocity measurements were taken at 0.4 m (1.3 ft), 1.1 m (3.6 ft), 1.5 m (4.9 ft) and 2.6 m (8.5 ft) from the left rib, and at heights of 0.6 m (2 ft), 1.2 m (4 ft) and 1.6 m (5.5 ft) above the floor (Martikainen et al., 2011).

Construction of the computational model—The numerical models presented in this paper were developed using the commercial CFD software package ANSYS Fluent, Version 13. The constructed 3-D CFD model consists of two primary components: a long rectangular entry 1.9 m (6.2 ft) high, 2.9 m (9.5 ft) wide, and 60 m (197 ft) long, with a cart 2.6 m (8.5 ft) long, 0.95 m (3.1 ft) wide and 1.2 m (4 ft) high acting as an obstruction located 20 m (66 ft) from the left inlet of the entry (Fig. 3). A constant inlet or incident velocity condition of 1.2 m/s (236 ft/min) in the horizontal direction was applied at the inlet. The pressure outlet boundary condition was applied at the outlet, while the wall boundary was treated using a wall-function approach. Turbulence models, including standard k-epsilon, RNG k-epsilon, and SST k-omega were evaluated for this specific model. Because differences in the results of these approaches were slight, the results presented in this paper are based on the more common standard k-epsilon treatment.

Comparison of experiment data and simulated data—Figure 4 shows the CFD-simulated velocity distribution 3 m downstream of the obstruction, which corresponds to the measurement plane in Fig. 2. Also shown are the locations where the air velocity measurements were collected during the underground study.

Figure 5 compares the thirteen measured air velocities and their CFD-simulated values shown in Fig. 4. Considering the good agreement between the two sets of data, it appears that the CFD model agrees well with the experimental test results at location 1. In other words, the CFD model has been successfully validated in this specific case and thus can be used for further studies related to the obstruction investigation.

CFD model for the larger-sized entry—The NIOSH Bruceton Experimental Mine, where the underground obstruction experiments were conducted, was developed in the 1910s for testing of gasoline locomotives, mining machinery, explosives, electrical equipment and ventilation methods. The 2.7-m (9-ft) entry width is much smaller than the 4.5-m (15-ft) to 6.0-m (20-ft) widths currently found in modern coal mines. Therefore, in the CFD model, the entry size was scaled up to a more typical width of 5.5 m (18 ft) and a height of 2.4 m (7.8 ft). The new CFD model for the larger entry size retains all relevant configurations including cart size, meshing size, boundary conditions and turbulent model design. All results and discussion presented in the next section refer to the larger entry size unless otherwise indicated.

Results and discussion

Wake zone downstream of the obstruction

The CFD simulations provide insight into the effects of the obstruction on the profile of the downwind airflow. A profile of velocity *u* around the obstruction at the centerline plane of the entry (z = 2.75 m) is given in Fig. 6. For the physical flow of fluid past an obstruction, experimental observations indicate that the flow generally separates at certain points on the obstruction, creating a highly turbulent region behind the object, called the wake (Wu, 1961). The occurrence of three wake zones in the area behind the cart, in the foot board and in the region behind the cart seat back, can be seen from the plot of velocity contours and vectors in the CFD simulations. This figure indicates a circular cavity of relatively slow moving air on the downwind side of the obstruction.

A wake is characterized by negative pressure within its boundary and the presence of inefficient mixing with outside airflow. The effects of a wake weaken with increasing distance from an obstruction. In a free stream, such as a building in the atmosphere, the height of the wake region often extends up to about 2.5 times the height of the obstruction and extends downwind upwards to 10 times the height of the obstruction (APTI, 2011). A similar scenario with the wake zones extending above and behind the cart can be seen in Fig. 6. As demonstrated in the figure, it is also apparent that the downstream effects of obstructions are much more pronounced than the upstream effects.

Factors affecting measurement site selection downstream of an obstruction

The obstruction size, the entry size and even the initial airflow velocity can affect the size and extent of the wake zones and, consequently, the minimum measurement distance downstream of an obstruction. The following CFD models were constructed to study the impact of these factors.

1) Entry size—In the recommendations given by Kohler and English (1983) and Thimons and Kohler (1985) regarding selection of an airflow measurement site downstream of an obstruction, the entry size or, more accurately, the entry diameter, was the only element considered. It is apparent that the entry size could affect the minimum downstream distance. Therefore, in this study, two comparable CFD models were constructed with different entry dimensions: 5.5 m (18 ft) wide by 2.4 m (8 ft) high, and 3.5 m (11 ft) wide by 1.9 m (6.2 ft) high. Incident or inlet velocity was 1.2 m/s (236 ft/min). Cart size, boundary conditions and initial conditions were the same as in the previous analysis.

The velocity contours illustrated in Fig. 7 demonstrate that entry size has a significant influence on the extent of the wake zone. They are plotted out at the plane 0.6 m (2 ft) above the floor of the entry, which is the centerline of the wake zone and where the wake zone reaches its furthest extent (Fig. 7). Minimum measurement distance should not be determined from plotted velocity contours. The actual point velocity values are needed to establish the location where minimal velocity change occurs with the presence of the obstacle. However, the sizes and extents of the wake zones are readily seen in this figure. Generally, a larger wake zone corresponds to a larger minimum measurement distance. A

smaller entry develops higher airflow velocities near an obstruction, but a larger entry shows a larger downstream wake. For a similarly sized obstruction, the wake zone and, therefore, the minimum measurement distance, increases with the entry dimensions.

2) Obstruction size—To investigate the impacts of obstruction size on the airflow patterns downstream of an obstruction, two sets of models were built based on the validated CFD model. The first two models studied the influence of the obstruction height on the airflow, with cart heights of 1.2 m (4 ft) and 2.0 m (6.6 ft), using entry dimensions of 5.5 m (18 ft) wide by 2.4 m (8 ft) high. The simulated velocity contours at the 0.6-m (2-ft) and 1.1-m (3.6-ft) planes above the entry floor, for the cart heights of 1.2 m (4 ft) and 2.0 m (6.6 ft), are presented in Fig. 8. With the increased obstruction height, this figure shows the increased length of the disturbed area downstream of the cart, as well as the higher airflow velocities on both sides of the cart.

The second model considered cart widths of 0.95 m (3.1 ft) and 2.95 m (10 ft) to assess the impact of obstruction width on airflow distribution. Entry dimensions, again, were 5.5 m (18 ft) wide by 2.4 m (8 ft) high, and the cart was 1.2 m (4 ft) high. Figure 9 shows that the wider cart produced a larger disturbed area downstream of the cart. A maximum velocity of 1.90 m/s (374 ft/min) was obtained with the wider cart, compared to a lower velocity of 1.40 m/s (276 ft/min) with the narrower cart. These simulation results illustrate that the obstruction size can have a significant impact on the extent of the wake zone downstream of the obstruction and, therefore, on the minimum measurement distance.

3) Inlet velocity—Numerical calculations were made for inlet flow velocities of 0.5 m/s and 5 m/s to study the impacts of this factor on the distribution of airflow around the cart. For this analysis, entry size was 5.5 m wide by 2.4 m high and the cart was 1.2 m high by 0.95 m wide. Comparing the two plots of horizontal velocity at the centerline plane for an inlet or incident velocity of 0.5 m/s (top) and 5 m/s (bottom), very similar velocity contours near the cart were obtained, and no differences were observed except that the magnitude of the velocity component increased (Fig. 10). Similar results regarding the impacts of velocity change were obtained by Naeeni and Yaghoubi (2007). The simulated velocity profiles for inlet airflow velocities of 0.5 m/s (98 ft/min) and 5 m/s (980 ft/min) led to the conclusion that the airflow velocity does not affect the flow pattern around an obstruction in an entry. Therefore, a variation in airflow velocity does not change the length of the disturbed area downstream of an obstruction. Thus, velocity can be ignored as a factor to determine the optimum measurement distance from an obstruction.

Criteria specifying the minimum downstream distance

The above studies have made it clear that the minimum measurement distance downstream of an obstruction is dependent upon the entry size and the obstruction size, but independent of the inlet velocity. With this knowledge, mine operators would benefit from guidelines to position air velocity measurement locations around an obstruction if a mathematical relationship could be developed between the minimum downstream distance and the entry size and obstruction size.

The configurations for all previously illustrated CFD models are shown in Table 1. Hydraulic diameters, a very common concept used in fluid dynamics, are employed to represent the sizes of the entry. The hydraulic diameter of the entry (D_H) can be calculated as shown in Eq. (1):

$$D_H = \frac{4A}{P} \quad (1)$$

where A is the flow area and P is the wetted perimeter defined as the perimeter of the cross sectional area in contact with the fluid body. The wetted perimeter of a ventilation entry equals the perimeter of the entry since it is full of air. For an obstruction in a fluid flow, the obstruction characteristic dimension (usually its hydraulic diameter) is used to represent its size (Raghunathan et al., 2002; Berthier and Silberzan, 2009). The hydraulic diameter of the obstruction (d_H) can be calculated with Eq. (1). Of particular interest is the idea of a minimum distance downstream from an obstruction where an airflow reading can be accurately made. To determine the minimum distance, the velocity along the centerline of the wake zone was plotted for each case in Table 1. The distance at which the velocity curve flattens was chosen as the minimum distance. The logic of this approach is that an airflow measurement made further away from the obstruction would be very similar to that found at the minimum distance, while a reading made closer to the obstruction would be more inaccurate due to the presence of eddies and vortices.

Given the above approach, if the variable Y is defined as the ratio of the minimum distance (L) to the hydraulic diameter of the obstruction (d_H), and X is defined as the ratio of D_H/d_H, then five datasets of Y and X can be plotted as shown in Fig. 12. A least squares regression produces the following expression relating X and Y:

$$Y = 3.3X + 10.0 \quad (2)$$

with $R^2 = 0.7$. Substituting Y and X into the relationship yields the minimum distance as a function of D_H and d_H:

$$L = 3.3D_H + 10d_H \quad (3)$$

The data in Table 1 show that the old recommendation specifying a minimum distance of 10 times the entry diameter generally overestimates this distance. This new relationship, as shown Eq. (3), specifies the minimum downstream distance for an air velocity measurement, considering the influence of both entry size and obstruction size.

Impact on the fixed-point air velocity sensor

When a mine ventilation network becomes very large and complex, remote monitoring of key parameters can provide first-hand knowledge of underground conditions. The continuous monitoring of air velocity in underground mining operations allows for fast recognition of changes and enables the mine operator to identify the occurrences of abnormal airflow levels. To this end, the fixed-point velocity sensor is usually mounted at a location in the entry to measure the air velocity for the long term. The likelihood that either

a stationary or moving obstruction such as equipment or personnel will be moved or be positioned near the measurement location is unavoidable. Therefore, the question arises as to whether a fixed-point air velocity sensor can detect the unexpected presence of personnel, machinery or even a roof fall.

To address this issue, a CFD model was created to assess the impacts of an obstruction on the readings of a fixed-point velocity sensor. An entry size of 5.5 m (18 ft) wide by 2.4 m (8 ft) high and cart dimensions of 1.2 m (4 ft) high by 0.95 m (3.1 ft) wide were again assumed. The impacts of the obstruction on the readings of a fixed-point velocity sensor mounted along the centerline of the entry at distances of 0.1, 0.2, 0.3, 0.4 and 0.5 m below the roof were simulated using CFD, and the results are shown in Fig. 12.

It is known that sensor locations closer to the roof may record lower velocities due to the viscous effects of the surface of the entry at the boundary layer. The results in Fig. 12 show that variations in velocity measurements above an obstruction can exceed 10% of the velocities upwind and downwind of the obstruction. The velocity increase was located in the interval from X = 20 m (66 ft) to 24 m (79 ft) in Fig. 12, which is not much larger than the cart itself. Unless the fixed-point sensor is located in the area above the obstruction, a very limited likelihood exists to detect a change in velocity given the rapid return to upstream velocity conditions.

Conclusions

A CFD model was built using Ansys/Fluent to investigate the impacts of an obstruction on the downstream distribution of airflow and to specify the proper positioning of a device to record airflow velocities. The model was successfully validated with experimental data that confirmed the agreement between the simulated and field results. Wake zones caused by the interaction of the airflow with the obstruction were clearly displayed. The size and extent of the wake zone downstream of an obstruction in an underground entry was affected by the entry size and the obstruction size.

Test results confirmed the results of other researchers—specifically, that inlet velocity did not affect airflow distribution around this obstruction. Of particular importance was the minimum distance at which an air velocity monitor could be placed to avoid airstream disruptions caused by the obstruction. Previous work specifying a minimum downstream distance of 10 times the entry diameter was found to be overly conservative. An analytical expression $L = 3.3D_H + 10d_H$ determined the minimum downstream distance as a function of both the entry size and the obstruction size.

The effects of the obstruction on the fixed-point velocity sensor were also considered. The output of a fixed-point velocity sensor was found to vary with the distance below the roof, while the obstruction influenced the sensor only over a very limited distance. In other words, the impacts of an obstruction on airflow velocity were only seen close to the obstruction, as velocities quickly returned to upstream levels after passing the obstruction.

There are many variously shaped obstructions, such as equipment, personnel, occasional roof falls and rib rolls, existing in underground mines. This study considered the impacts of

a regularly shaped obstruction on an airflow distribution for which experimental data was available. The shape effect on the airflow mostly occurred at near body range, and the general conclusions obtained in this paper will not vary significantly when applied to irregularly shaped obstructions.

Acknowledgments

The authors would like to recognize and thank Paul Gorder (CONSOL Energy), Thomas Morley (MSHA) and Randy Reed and Liming Yuan (NIOSH) for their valuable comments and suggestions to make this paper complete. The authors also thank Andrew Mazzella for assistance with the experimental data.

References

Aminossadati, SM.; Hooman, K. Numerical simulation of ventilation air flow in underground mine workings. In: Wallace, KG., editor. Proceedings of 12th U.S./North American Mine Ventilation Symposium. Reno; NV: 2008. p. 253-259.

APTI (Air Pollution Training Institute). 2011. http://www.shodor.org/os411/courses/411c/module04/unit04/page03.html

Berthier J, Silberzan P. Microfluidic for Biotechnology. Artech House. 2009:483.

Dhiman, A.; Hasan, M. CFD analysis of the steady flow across a tapered trapezoidal cylinder. Proceedings, World Congress on Engineering; London, U.K.. WCE 2010, June 30-July 2; 2010. p. 1094-1096.

Gong R, Bhaskar R. Three-dimensional mathematical modeling of airflow at a continuous miner face. AIME Transactions. 1992; 292:1888–1893.

Hargreaves DM, Lowndes IS. The computational modeling of the ventilation flows within a rapid development drivage. Tunneling and Underground Space Technology. 2007; 22:150–160.

Izadi, MJ.; Asghari, P.; Delakeh, MK. CFD study of the pressure distribution on the back of a 3-D bluff body (cube) of air flow in different Reynolds numbers. Proceedings of the ASME 2009 Fluids Engineering Division Summer Meeting; Vail, CO. August 2-6; 2009. p. 1399-1407.

Konno, N.; Mochida, A.; Maruyama, T.; Hagishima, A.; Tanimoto, J.; Kikuchi, A.; Kikuchi, Y. CFD prediction of turbulent flow under the influence of moving automobiles in street canyons. In: Hanjalić, K.; Nagano, Y.; Jakirlić, S., editors. Turbulence, Heat and Mass Transfer 6. Begell House, Inc.; 2009.

Kohler JF, English LM. Determination of Velocity Measurement Correction Factors and Guidelines. Final Report. 1983:216. USBM Contract No. J0308027.

Lu, JWZ.; Lun, IYF.; Lam, JC. CFD investigation of airflow around objects with different shapes. Proceedings of Building Simulation 1999; Kyoto, Japan. 1999.

Martikainen AL, Taylor CD, Mazzella AL. Effects of obstructions, sample size and sample rate on ultrasonic anemometer measurements underground. Preprint, Annual Mtg., Society for Mining, Metallurgy, and Exploration, Denver, CO. 2011

Meile W, Brenn G, Reppenhangen A, Lechner B, Fuchs A. Experiments and numerical simulations on the aerodynamics of the Ahmed body. CFD Letters. 2011; 3:32–39.

Naeeni N, Yaghoubi M. Analysis of wind flow around a parabolic collector (1) fluid flow. Renewable Energy. 2007; 32:1898–1916.

Raghunathan RS, Kim HD, Setoguchi T. Aerodynamics of high-speed railway train. Progress in Areospace Science. 2002; 38:469–514.

Sahini, D. Wind Tunnel Blockage Corrections: A Computational Study, Thesis. Texas Tech University; 2004.

Tavakol MM, Yaghoubi M. Experimental and numerical analysis of turbulent air flow around a surface mounted hemisphere. Transaction B: Mechanical Engineering. 2010; 17:480–491.

Thimons, ED.; Kohler, JL. Measurement of Air Velocity in Mines. US Bureau of Mines, Report of Investigations; 1985. p. 30

Wala AM, Taylor CD, Huang G. Mine face ventilation: a comparison of CFD results against benchmark experiments for the CFD code validation. Mining Engineering. Oct; 2007 59(10):49–55.

Wu TY. A wake model for free-streamline flow theory, Part I. Fully and partially developed wake flows and cavity flows past an oblique flat plate. Fluid Mech. 1961; 13:161–183.

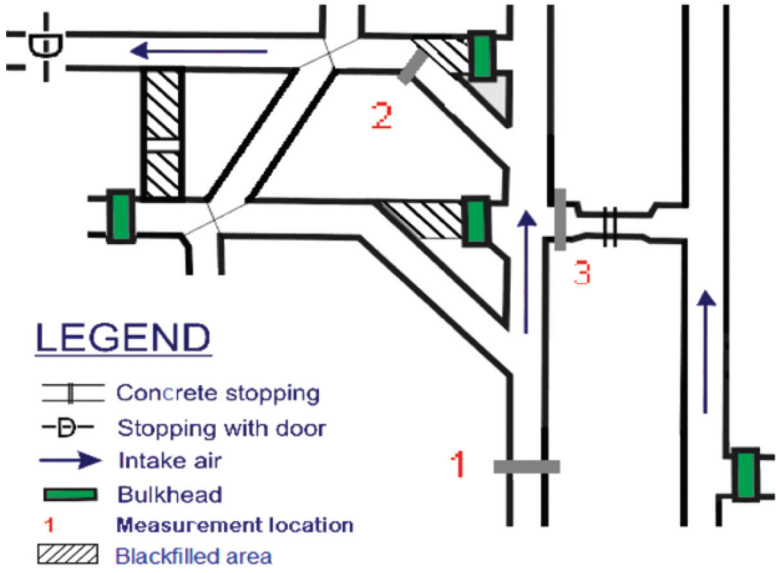

Figure 1.
Underground test locations at the NIOSH Bruceton Experimental Mine (after Martikainen et al., 2011).

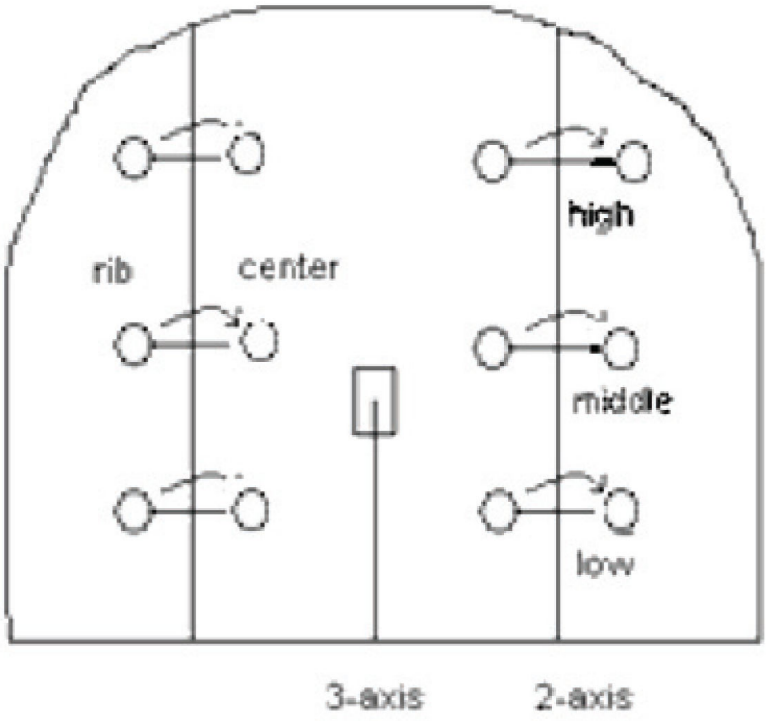

Figure 2.
Anemometer placement at Location 1 (after Martikainen et al., 2011).

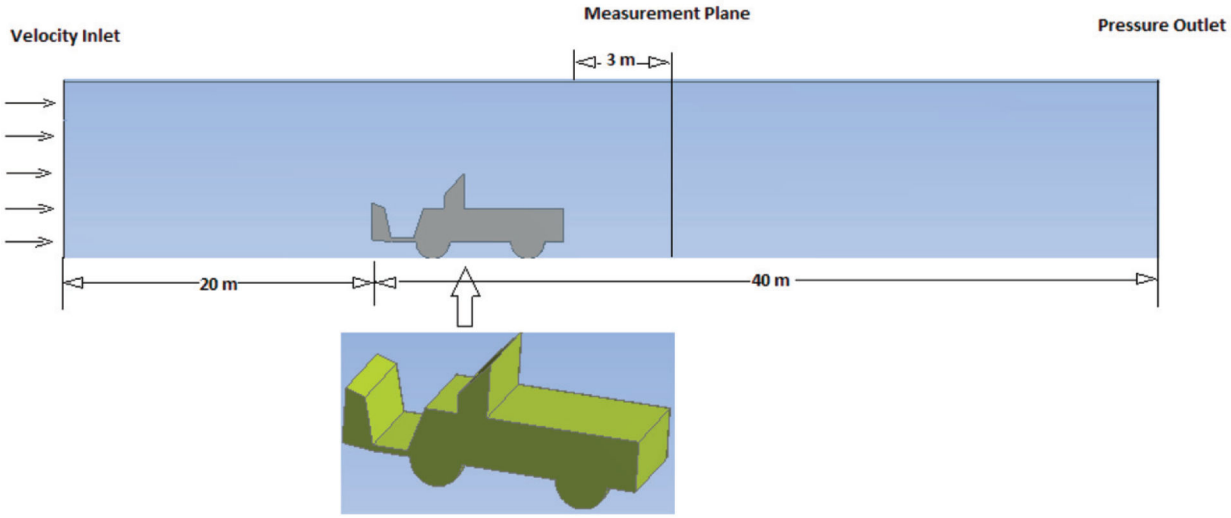

Figure 3.
Three-dimensional CFD model layout.

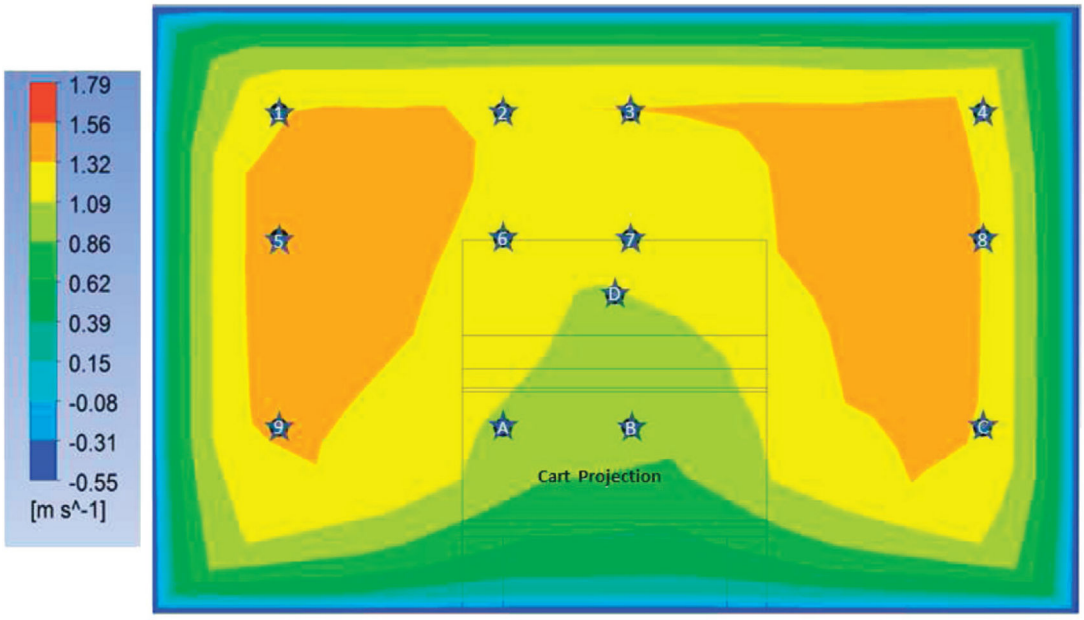

Figure 4.
Airflow distribution and air velocity measurement points 3 m downstream of the obstruction.

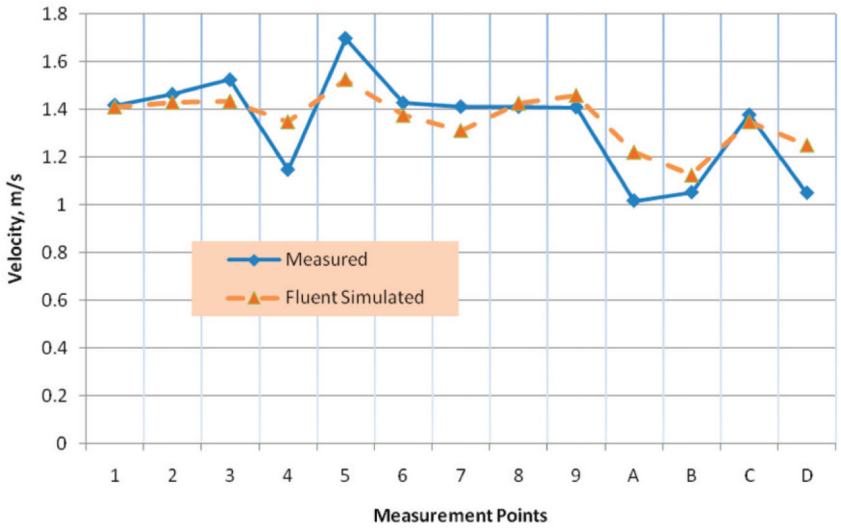

Figure 5.
Comparison of measured and simulated air velocity measurement points shown in Fig. 4.

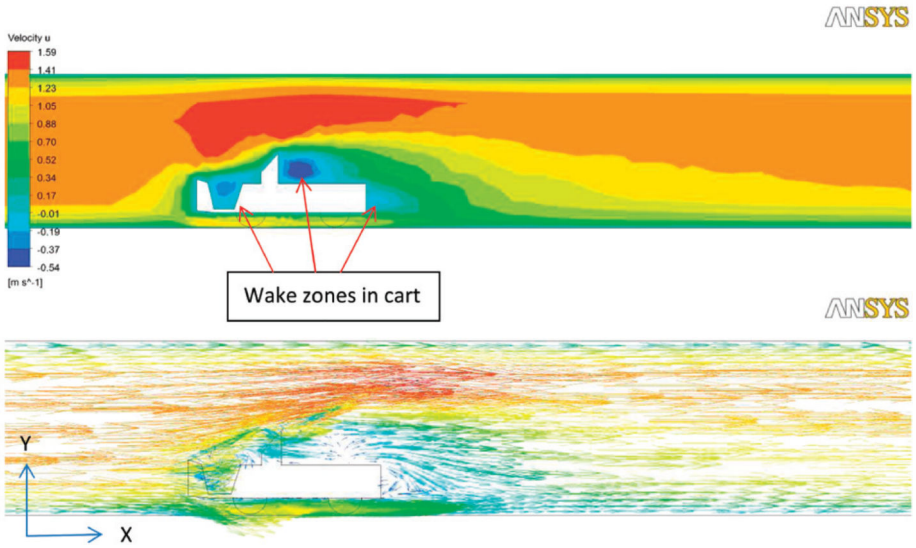

Figure 6.
Velocity contours (above) and velocity vectors (below) at the centerline plane.

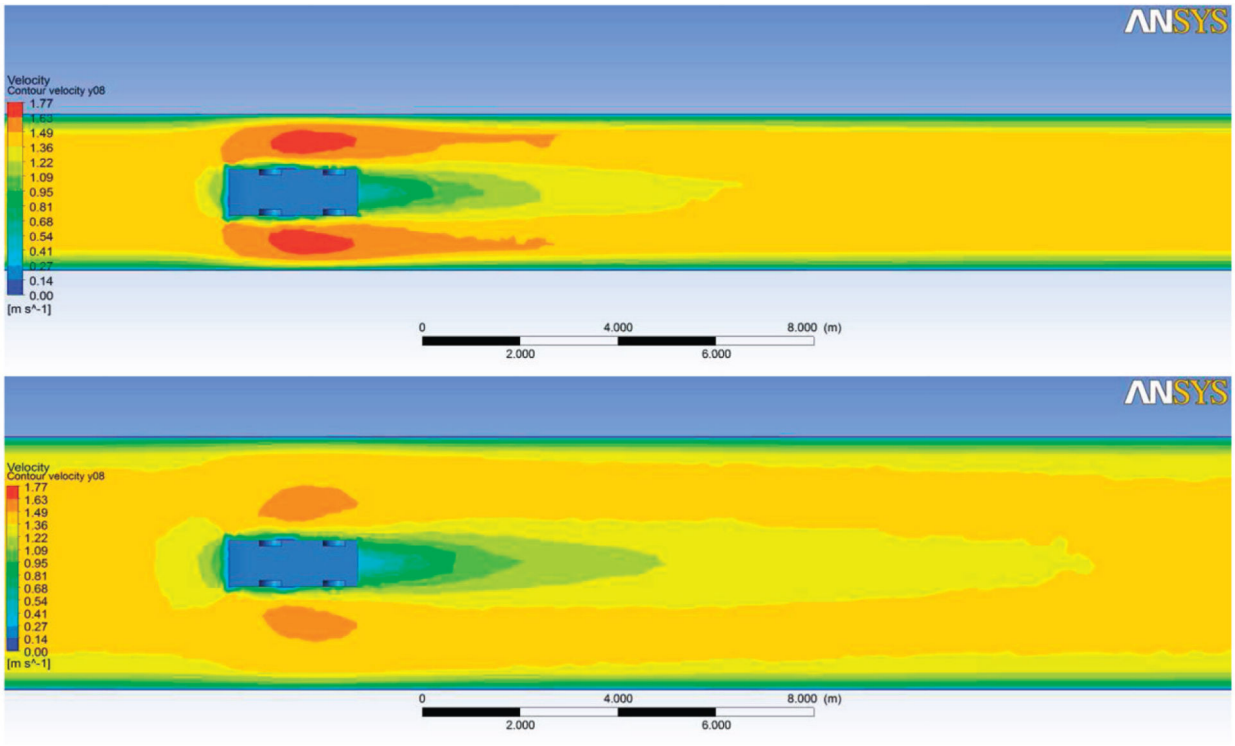

Figure 7.
Velocity contours for the 3.5-m-by-1.9-m entry (top) and the 5.5-m-by-2.4-m entry (bottom).

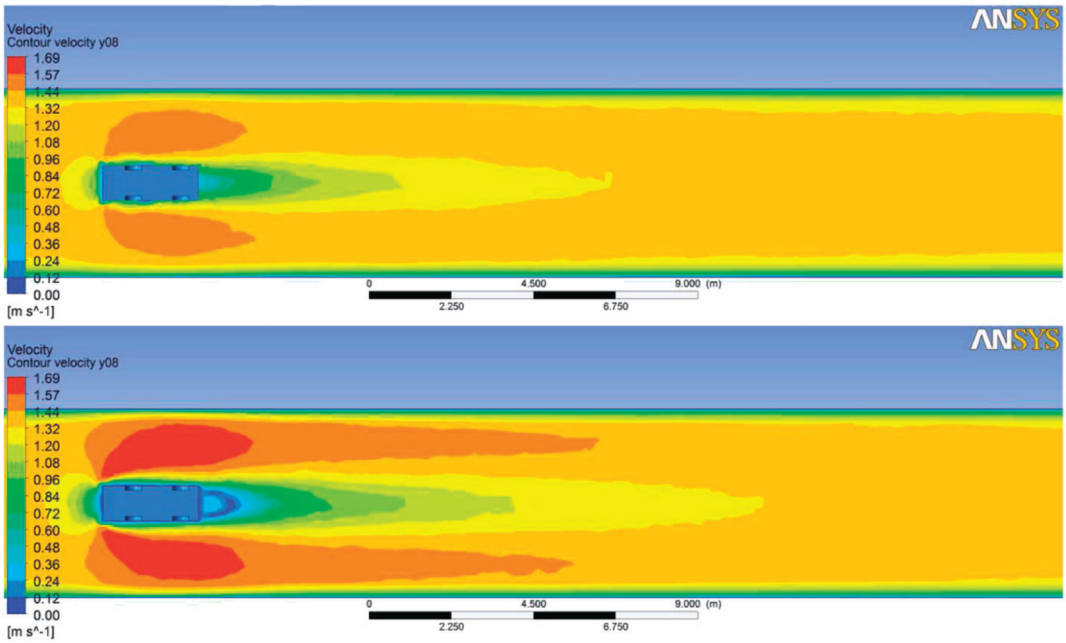

Figure 8.

Velocity contours with a cart height of 1.2 m at the plane $y = 0.6$ (top) and with a cart height of 2.0 m at the plane $y = 1.2$ m (bottom).

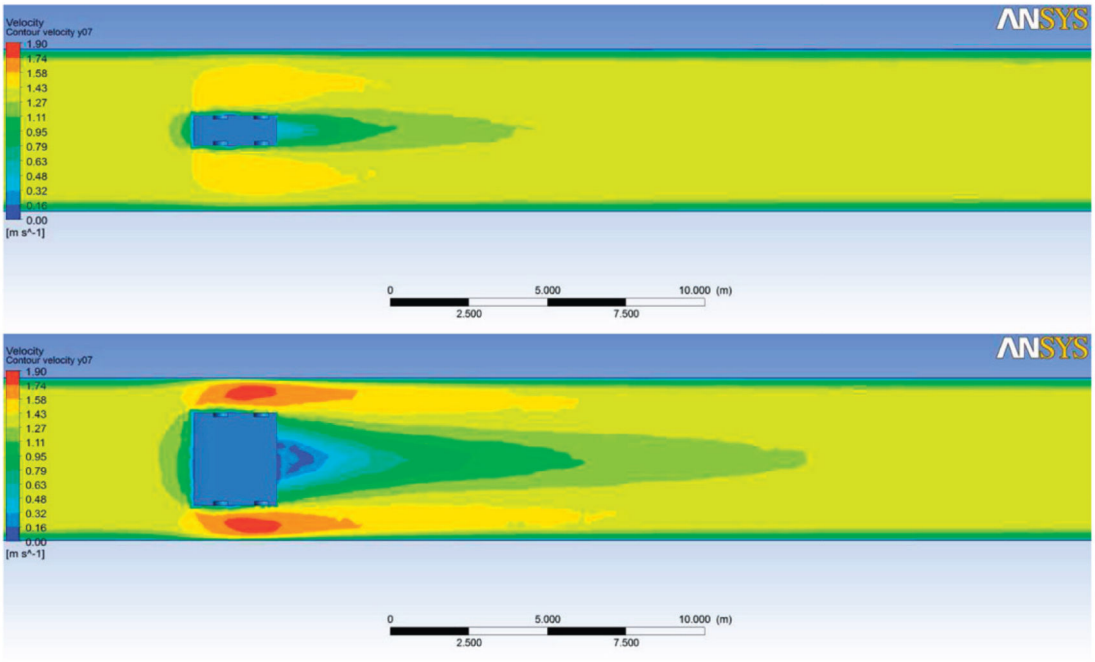

Figure 9.
Velocity contours with cart widths of 0.95 m (top) and 2.95 m (bottom) at the plane $y = 0.6$ m.

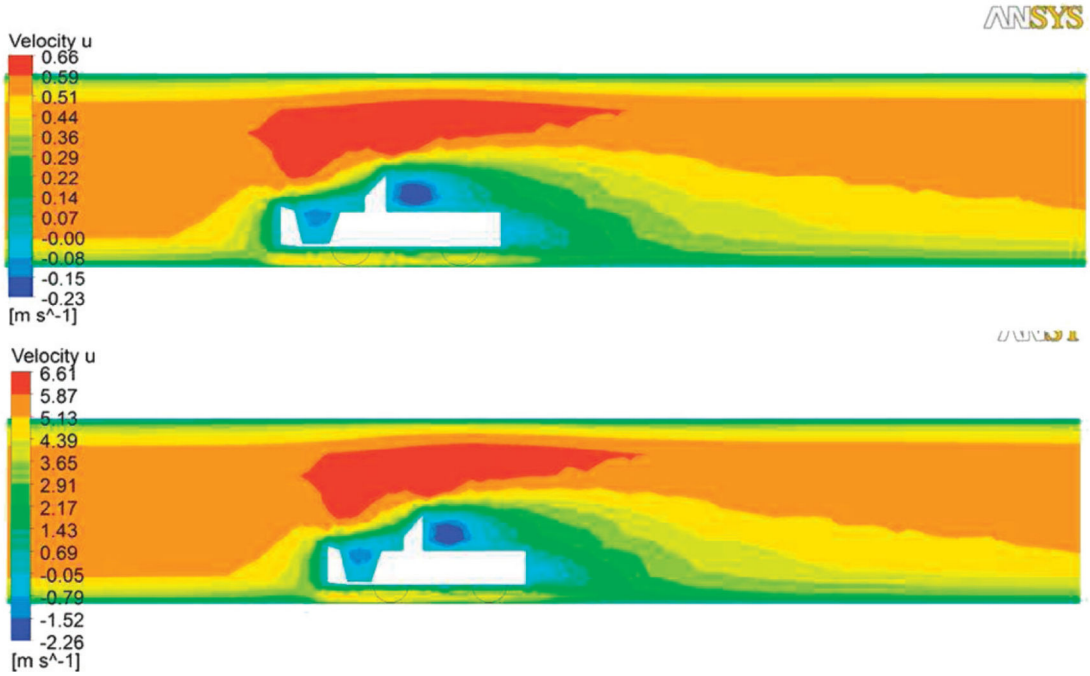

Figure 10.
Velocity contours at a central plane for an inlet velocity of 0.5 m/s (top) and 5 m/s (bottom).

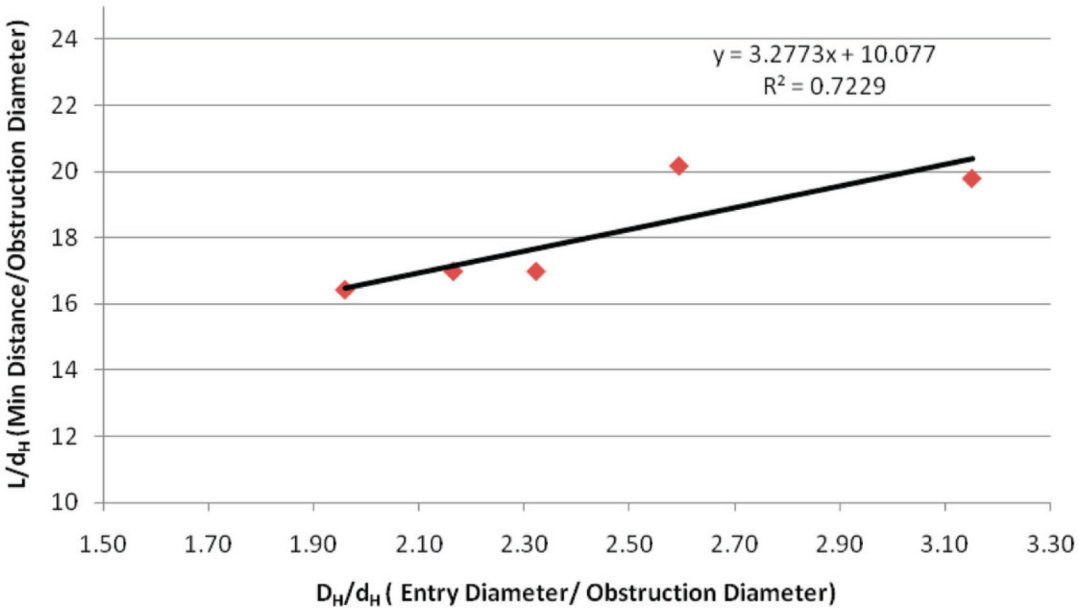

Figure 11.
Regression of L/d_H on D_H/d_H.

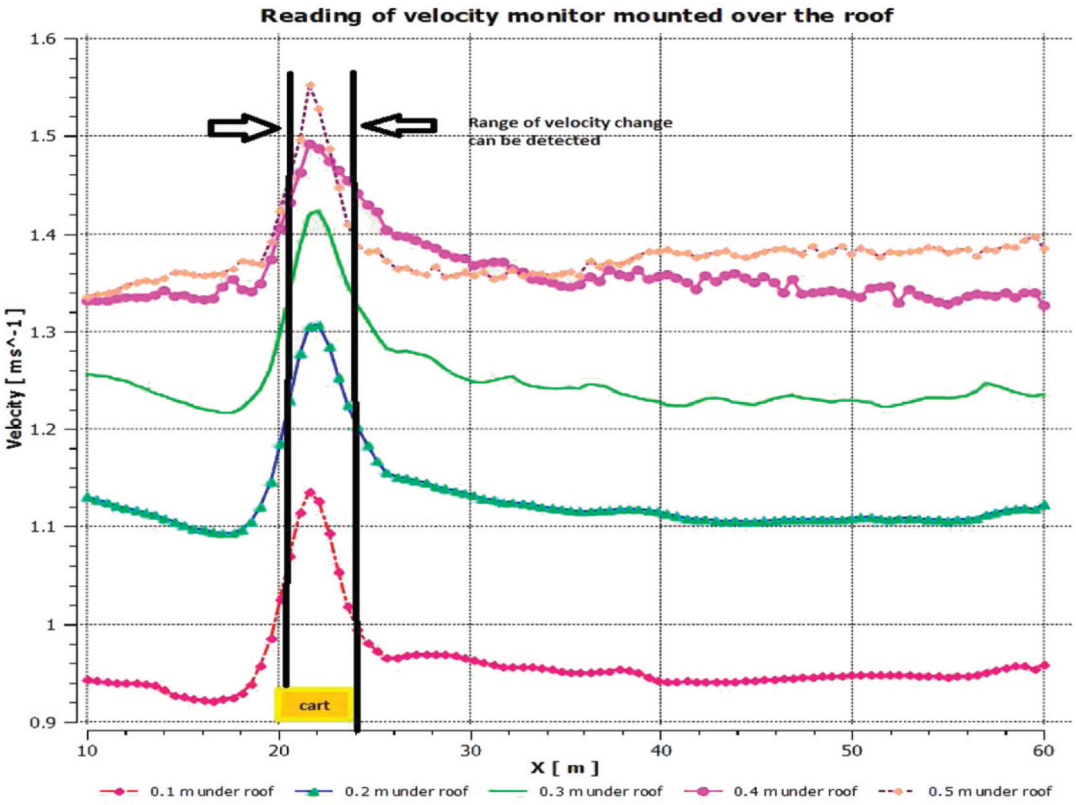

Figure 12.
Comparisons of the virtual fixed-point velocity sensor readings for various mounting distances below the roof.

Table 1

Data for entry size, obstruction size and minimum distance (unit: m), based on configurations for all previously illustrated CFD models.

Entry			Obstruction			Min. Distance
Width	**Height**	D_H	**Width**	**Height**	d_H	
5.50	2.40	3.34	0.95	1.2	1.06	21
5.50	2.40	3.34	0.95	2	1.29	26
5.50	2.40	3.34	2.95	1.2	1.71	28
3.50	1.90	2.46	0.95	1.2	1.06	18
2.90	1.90	2.30	0.95	1.2	1.06	18